Heliyon 10 (2024) e29540

Contents lists available at ScienceDirect

Heliyon

journal homepage: www.cell.com/heliyon

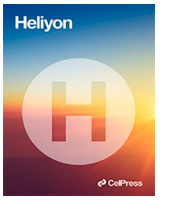

Research article

Feasibility analysis of inactivating influenza A(H1N1) virus using UVC robot in classroom environment

Yizhen Wu [a], Peiyao Guo [a], Dekun Luo [a], Jianyu Deng [a], Huilu Yao [a], Wenhong Sun [a,b,c,*]

[a] Research Center for Optoelectronic Materials and Devices, Guangxi Key Laboratory for the Relativistic Astrophysics, School of Physical Science & Technology, Guangxi University, Nanning 530004, China
[b] MOE Key Laboratory of New Processing Technology for Nonferrous Metals and Materials, Guangxi Key Laboratory of Processing for Non-ferrous Metals and Featured Materials, Nanning 530004 Guangxi, China
[c] Third Generation Semiconductor Industry Research Institute, Guangxi University, Nanning 530004, China

ARTICLE INFO

Keywords:
Influenza A
Influenza A virus
Deep ultraviolet LED
Robot
UVC
Virus inactivation
Robot technology
Classroom environment

ABSTRACT

Background: Starting from 2009, H1N1 has been one of the respiratory diseases that afflict the global population. Concurrently, due to the influence of COVID-19, it has become widely accepted that preventing the virus's spread necessitates personal protection measures and disinfection in public spaces.
Experiments: This study conducted two experiments. In the classroom experiment, six UVC dose test points were calibrated to test whether the UVC dose at each testing point met the standards for inactivating IAVs and the time required to meet the standards. In the simulated classroom experiment, seven square slides made of IAVs were placed. After 10 min of robot movement, irradiated sterile square slides were made into suspension and injected into chicken embryos. Cultivate chicken embryos and conduct IAVs testing.
Results: Classroom experiment has shown that 5 testing points can meet the standards for inactivating IAVs(3 mJ/cm^2), with a required time of 80 min, 40 min, 15 min, 5 min and 10 min. The UVC dose for testing points that do not meet the standards in 80 min is only 0.5 mJ/cm^2. The simulation classroom experiment outcomes revealed that 99.99 % of IAVs were deactivated. Furthermore, this study established both a desktop control group and a chair arm control group, both of which yielded identical results, indicating an inactivation logarithm of IAVs≥4log.
Conclusion: The study presented that IAVs on the surface of an object can be effectively and rapidly deactivated at an irradiation density of 1.8 mW/cm^2. Meanwhile, the study provides evidence of the feasibility of using the GXU robot to inactivate IAVs in a classroom environment.

1. Introduction

Respiratory illnesses stemming from respiratory pathogens have garnered global attention. Following the H1N1 pandemic in 2009, the influenza A virus (IAVs) has extensively circulated worldwide, imposing a significant strain on the healthcare systems of various nations. As of August 1, 2022, statistics from the China Bureau for Disease Control and Prevention indicate that H1N1 has led to over

* Corresponding author.
E-mail address: youzi7002@gxu.edu.cn (W. Sun).

https://doi.org/10.1016/j.heliyon.2024.e29540
Received 17 July 2023; Received in revised form 6 April 2024; Accepted 9 April 2024
Available online 15 April 2024

1.5 million hospitalizations and caused three fatalities, resulting in a mortality rate below 0.01 % [1]. During that year, the Centers for Disease Control and Prevention (CDC) in the United States made a projection of over 9 million instances of influenza and approximately 20,000 fatalities occurring between 2021 and 2022 [2]. Despite its low mortality rate, the high contagiousness and pathogenicity of H1N1 emphasize the continued importance of preventing and managing the transmission of influenza A viruses (IAVs).

Within the realm of respiratory diseases, there are three prevalent modes of transmission: droplet transmission, aerosol transmission, and airborne transmission [3,4]. H1N1, a respiratory pathogen disease, primarily spreads through direct or indirect contact between individuals [5]. Direct contact with the oral or nasal secretions of an infected person can result in virus transmission [6]. Similarly, there is a higher likelihood of infection through indirect exposure, such as inhaling or touching the droplets or respiratory secretions of an affected individual [7]. Moreover, influenza A viruses (IAVs) have the ability to swiftly contaminate surfaces, particularly in densely populated settings like hospitals, schools, and nursing homes. Once an infection occurs, IAVs can rapidly propagate [4,8]. Therefore, effectively preventing the spread of IAVs entails thorough cleaning and disinfection of object surfaces [7].

Ultraviolet (UV) radiation is a widely employed method for eradicating microorganisms. When microorganisms are exposed to UV radiation, their cellular structures are compromised, hindering their replication and ultimately leading to microbial death [9–12]. Influenza A viruses (IAVs) belong to the RNA virus category and consist of eight segments of single-stranded RNA genome along with lipid and carbohydrate components [13]. Numerous reports have demonstrated the effectiveness of UV radiation in inactivating IAVs. For instance, Devin Mills et al. [14] observed a significant reduction (≥3log) in IAV activity when N95 masks contaminated with IAVs were treated with Ultraviolet Germicidal Irradiation (UVGI) and reported that the activity of IAVs was significantly reduced (≥3log) after the N95 mask contaminated by IAVs was treated with Ultraviolet germicidal irradiation (UVGI). Another study by Kojima M et al. [15] conducted UV light experiments using eight different wavelengths (365, 310, 300, 290, 280, 270, 260, and 254 nm) and found that the highest inactivation rate for the H1N1 subtype of IAVs was achieved with UV light at 260 nm. Furthermore, David Welch et al. [16] reported that far UVC light at 222 nm can deactivate over 95 % of atomized H1N1 influenza virus at a low dose of 2 mJ/cm^2. Additionally, K. Narita et al. [17] demonstrated that under the irradiation of far ultraviolet light (222 nm) at a radiation dose of 6 mJ/cm^2, IAVs were undetectable. Although these studies have illustrated the potential of UV radiation in inactivating IAVs, there is limited research on real-world applications of IAV inactivation using UV radiation.

In the context of the COVID-19 pandemic, the utilization of deep ultraviolet robots (UVC robots) has emerged as a promising solution for mitigating the challenges associated with manual disinfection. However, it remains uncertain whether UVC robots can effectively deactivate pathogens in more complex settings, such as school classrooms. Thus, this study introduces a novel deep ultraviolet robot (GXU Robot) equipped with automatic navigation and eight 273 nm ultraviolet lamps, providing a 360° irradiation range. Also, two experiments were conducted in this study, a classroom experiment and a simulated classroom experiment. The feasibility of the GXU robot to inactivate IAVs in a classroom environment was evaluated based on test results from two experiments.

2. Prior work

2.1. UVC lamp production

In contrast to previous experiments utilizing deep UV robots [4,18–21], the GXU Robot employed in this study is equipped with eight self-made 273 nm ultraviolet lamps, as illustrated in Fig. 1(a). Each lamp incorporates 24 high-power UVC beads, connected in both series and parallel configurations. Utilizing an Ultraviolet Detector (ATA-500UV) test, it was observed that when the current is set at 500 mA, the UVC bead achieves a maximum optical power of 80 mW, as depicted in Fig. 1(b). Once the GXU Robot is operational (powered by a 36 V, 32AH battery), measurements of the current during the robot's operation indicate that the maximum optical power of a single UVC lamp is estimated to be approximately 1.6 W, as shown in Fig. 2(b) through multiple measurements.

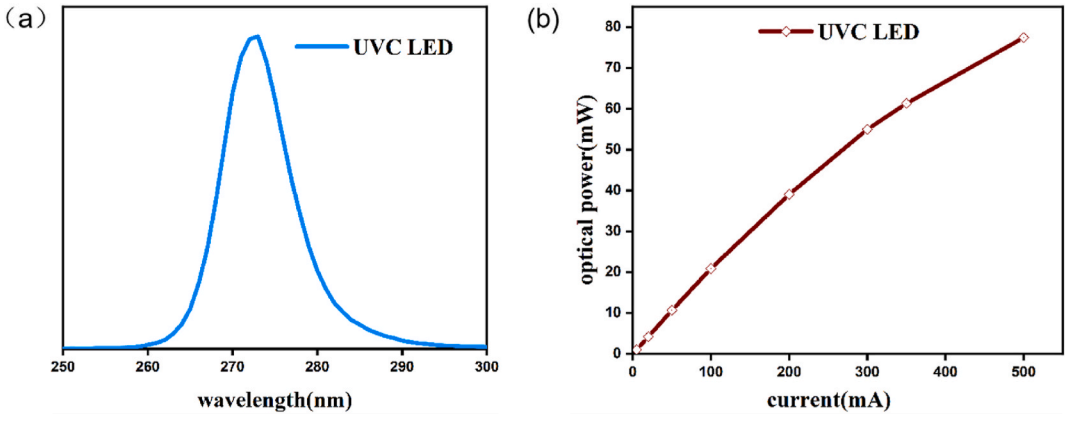

Fig. 1. (a) UVC bead wavelength curve. (b) Curve of optical power of the UVC bead changing with current.

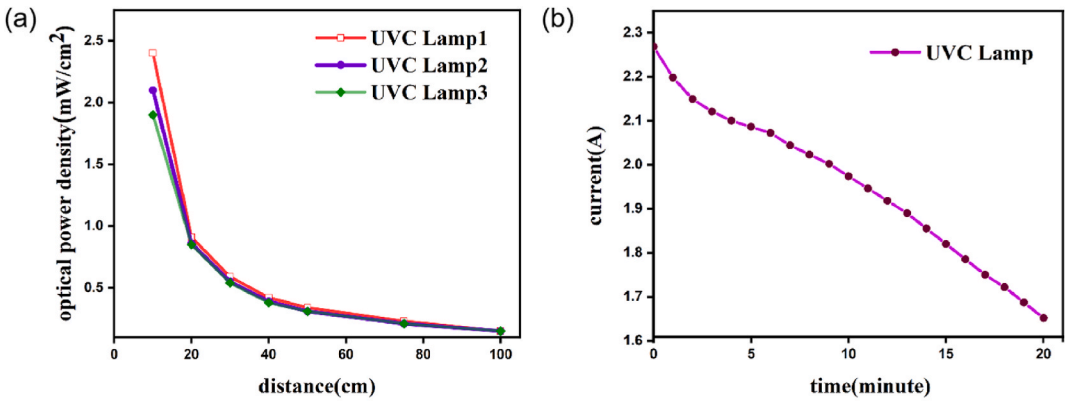

Fig. 2. (a) Attenuation curve of optical power density with distance of three UVC lamps (36 V, 2 A). (b) The Curve of UVC lamp current with time, when the robot works normally.

2.2. Attenuation of optical power density

The self-made UVC lamps utilized in this study exhibit a relatively low luminous efficiency, estimated to be approximately 3 %. In comparison to common low-pressure mercury lamps, the optical power density of the self-made UVC lamps decays at a faster rate with increasing distance. To investigate the attenuation of optical power in the self-made UVC lamps, an experiment was conducted to examine the changes in optical power density over varying distances (0–1 m). For the experiment, three out of the eight UVC lamps installed on the GXU robot were randomly selected for testing. The entire experiment was conducted in an environment devoid of any interference from other light sources. The LS125 multi-probe ultraviolet irradiance meter (LS125-UVC-X0 probe, with a spectral response of 230–280 nm, manufactured by Linshang Technology, Shenzhen, China) was positioned facing the UVC lamps. The experiment employed a 48 V power supply, with the UVC lamps illuminated for 30 s, followed by measurements taken using the LS125 multi-probe ultraviolet irradiance meter. The obtained data reveals the attenuation of optical power density in the three self-made UVC lamps with respect to distance, as depicted in Fig. 2(a). It is noteworthy that all three UVC lamps exhibit a consistent trend of attenuation. At a distance of 20 cm, the optical power density is reduced by half, and at 1 m, it is essentially negligible.

2.3. Deep ultraviolet robot

In this study, the deep ultraviolet robot (GXU Robot) utilizes the Athena universal robot development platform (Athena, model N4M11), which incorporates SLAM Technology, Fig. 4(a). The Athena platform integrates various sensors, including laser radar, ultrasonic sensors, and collision sensors. These sensors enable autonomous intelligent navigation and obstacle avoidance capabilities. The dimensions of the GXU Robot are 41 × 39 × 80 cm (length, width, and height). It is equipped with eight self-made UVC lamps (273 nm) that are each 1.2 m in length. These eight lamps are arranged in a rectangular configuration, allowing for a 360° irradiation

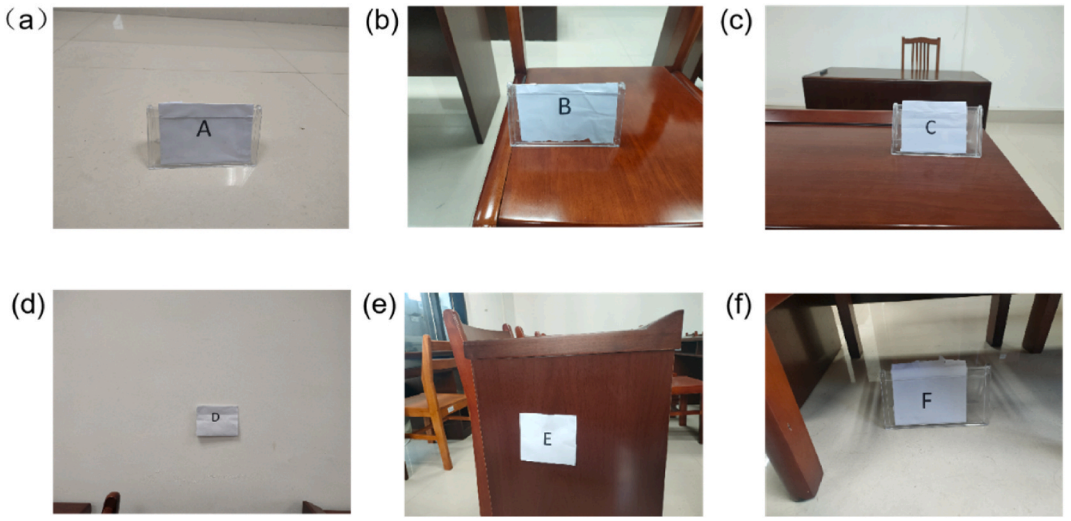

Fig. 3. (a) Floor. (b) Chair surface. (c) Desktop. (d) Wall. (e) On the side of the table. (f) At the bottom of the table.

coverage. In this study, the control of GXU robot was completed by a mobile app (GXU Robot app). GXU Robot app is an app developed based on Android software, suitable for mobile phones under the Android 12 system. The app was developed independently by our team and has not been published on public networks. The app and its tutorial can be obtained by contacting the author or corresponding author.

3. Experimental results and discussion 1

The GXU robot described in this study is specifically designed for classroom environment disinfection and sterilization. In comparison to corridors, halls, and conference rooms, the classroom environment is more complex. Therefore, in order to evaluate the feasibility of using the robot in actual classrooms, UVC dosage was tested in a university classroom. The classroom has an area of 50 m^2. Six testing points were placed in the classroom, as shown in Fig. 3(a)-(f). Measure the UV dose at six testing points during the robot's movement to verify whether the H1N1 virus inactivation dose (3 mJ/cm^2) is met, and record the time required for inactivation.

After the robot scans the classroom, it obtains a scanned map and adds 10 position points to the scanned map. Use the robot control app (GXU Robot app) to add work tasks and set the motion path, which are determined by 10 added position points. And then the robot begins to move as illustrated in Fig. S1 and Supplementary Video, the time required to complete the task is 5 min. The distance between the 6 testing points and the robot's movement is approximately 20 cm. The test results are shown in Table 1. The time required to reach the inactivation dose of IAVs (3 mJ/cm^2) at 5 test points, including the ground, chair surface, desktop, wall, and on the side of the table, is 80 min, 40 min, 15 min, 5 min, and 10 min, respectively. When the ground testing point reaches the minimum dose, the UVC dose at the bottom of the table is only 0.5 mJ/cm^2, much lower than 3 mJ/cm^2. Through this experiment, it has been proven that GXU Robot can achieve the UVC dose required to inactivate IAVs. However, further research is needed to determine whether the robot can truly inactivate the IAVs in the classroom environment.

4. Experimental results and discussion 2

4.1. H1N1 virus

The specific viruses used in this study were influenza A viruses (IAVs, ATCCVR-1496), provided by Ingalls Detection Technology Services (Shanghai) Co. First, IAVs was diluted 1:100 with 500 mL virus culture medium (DMEM, 1 % bovine serum albumin, antibiotic) and inoculated in a 96-well cell plate containing 3×10^4/well MDCK cells. Then, 146 μL of diluted virus solution was added to each of the 4 wells in the first column of the 96-well cell plate, and 100 μL of virus culture solution was added to each well in the other columns. Using a multichannel spiker, 46 μL of liquid was pipetted from the first well into the second well, and then diluted semi-logarithmically into the fifth well, 10^{-2}, $10^{-2.5}$, 10^{-3}, $10^{-3.5}$. Each well contained 100 μL of virus solution. Finally, cell lesions were stopped and the erythrocyte agglutination titer of IAVs was detected. When the hemagglutination concentration of IAVs was 1:640, dilutions of IAVs were applied to 10 × 10 mm sterile square slides for use in mock classrooms. The remaining IAVs dilutions were stored at −80 °C.

4.2. Experimental process

The research described in this paper was carried out in a simulated classroom scene within a small conference room, which had an area of approximately 30 m^2. A total of 24 sterile square slides, each measuring 10 × 10 mm, were prepared. These slides were coated with IAVs dilution with a hemagglutination concentration of ≥1:640. During the experiment, the GXU Robot irradiated twenty-one out of the 24 sterile square slides containing the dried IAVs for a duration of 10 min. Each test included both a positive control group and a negative control group. The negative control group consisted of culture plates containing normal saline, while the positive control group comprised sterile square slides with IAVs that had not been exposed to the GXU Robot's irradiation. The entire test was conducted three times to ensure reliability and consistency of the results.

During each experiment, a total of seven sterile square slides were strategically placed within the small conference room, which

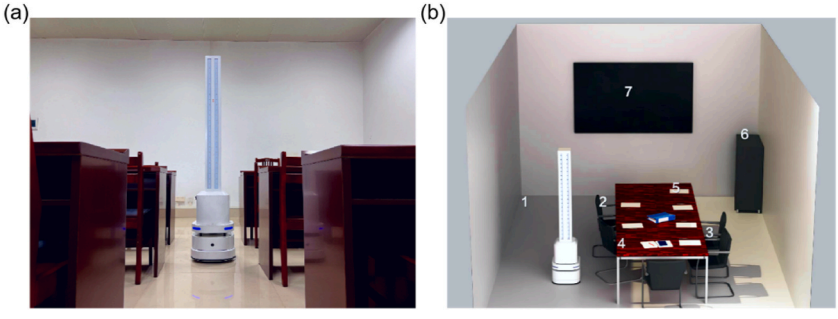

Fig. 4. (a) Self-made GXU Robot running in real classroom. (b) The self-made GXU Robot runs in the small office of the simulation classroom. The numbers 1–7 indicate the location of the sterile square slide of IAVs.

Table 1
Height of each test point and time required to reach a dose of 3 mJ/cm^2.

Testing points	Time required to reach a dose of 3 mJ/cm^2 (minute)	Height from ground (cm)
Floor	80	0
Chair surface	40	45
Desktop	15	75
Wall	5	105
On the side of the table	10	35
At the bottom of the table	80 minutes, the dose is 0.5 mJ/cm^2	0

served as a simulation of a classroom setting. These seven test points included the floor, the top of the cabinet, the blackboard, table top 1, table top 2, chair armrest 1, and chair armrest 2. The blackboard, positioned in the middle of the conference room, was located 1.7 m above the ground and corresponded to the topmost point of the GXU Robot. Adjacent to the blackboard, the cabinet was situated in the lower-left area, approximately 1.4 m high. The floor placement point was positioned in the lower-right section of the blackboard. As for table top 1, table top 2, chair armrest 1, and chair armrest 2, they were placed directly in front of the blackboard, as depicted in Fig. 4 (b). The movement of the GXU Robot is controlled by the GXU Robot app. Before starting the experiment, calibrate 7 position points on the main interface of the GXU Robot app, corresponding to the 7 numbers in Fig. 4(b), but with a distance difference of 20 cm. After the experiment starts, set the number of tasks through the GXU Robot app and move them for 10 min based on the calibrated position points. The time required to complete a task is 1 min. The movement steps are similar to Experimental results and discussion 1.

4.3. IAVs detection

After 10 min of irradiation by the GXU robot, 7 sterile square glass slides were added to 1 mL deionized water for the experiment. After repeated shaking, they were appropriately diluted with physiological saline, and then the diluted H1N1 virus was inoculated into chicken embryos. The method was as follows: Select 9–11 days old white shell chicken embryos (SPF grade), place the air chamber of the chicken embryos facing upwards on the egg tray, disinfect the chicken embryos with 70 %–75 % alcohol, and drill holes at the end of the air chamber to obtain a 10 × 6 mm crack. Take 0.2 mL of diluted IAVs solution using a syringe with a No. 16 needle, drop sterile liquid paraffin into the crack, gently shake the chicken embryo, and spread the liquid paraffin on the inner layer of the chicken embryo shell membrane. Then insert the injection needle into the chest of the chicken embryo, gently flick the chin and legs with the needle. When entering the amniotic cavity, the chicken embryo can be seen moving with the movement of the needle, and then inject 0.1 mL of solution for injection. Withdraw the needle to 1/2 inch and inject the remaining 0.1 mL solution into the allantoic cavity of the chicken embryo. According to the above method, use the same syringe to inoculate the diluted IAVs solution into two other chicken embryos.

At the same time, the positive control group containing sterile square slides containing IAVs placed in the natural environment and the negative control group injected with physiological saline into the allantoic cavity of chicken embryos were repeated to obtain 6 chicken embryos. Classify the various obtained chicken embryos, seal the cracks with sterilized medical tape, and place the chicken embryos with the air chamber facing upwards in a humidified incubator at a temperature of 35 °C for 2–3 days of cultivation. It is necessary to check the normal growth of chicken embryos every day.

4.4. Results and discussion

The results of the IAVs inactivation experiment conducted in this study are presented in Table 2, Table 3 and Table 4. Three chicken embryos were cultured in each of the three experiments, and they were directly inoculated with normal saline. The test results of the collected allantoic fluid showed negative for the presence of the virus. In the positive control group, where the deep ultraviolet robot irradiation was not applied, the virus titers were 5.76, 5.50 and 5.67, respectively. The difference between the three experimental results was less than 0.3, satisfying the statistical requirements for experimental data.

In this study, a fixed distance of 20 cm was maintained between the deep ultraviolet robot and the test samples. The samples were positioned at various heights, ranging from the ground to the 1.7 m blackboard, which corresponds to the height of the deep ultraviolet robot. The experimental results demonstrate that the deep ultraviolet robot achieves rapid and highly effective inactivation of IAVs within a short duration of exposure. Although the ground sample points exhibited a relatively lower rate of IAVs inactivation compared

Table 2
Results of the first inactivation test IAVs.

Sample location	Deactivation logarithm, log R	Inactivation rate, %	EID50
Wall	>4.00	>99.99	5.76
Top of cabinet	>4.00	>99.99	
Table top 1	>4.00	>99.99	
Table top 1	>4.00	>99.99	
Chair armrest 1	>4.00	>99.99	
Chair armrest 2	>4.00	>99.99	
On the floor	4.00	99.99	

Table 3
Results of the second inactivation test IAVs.

Sample location	Deactivation logarithm, log R	Inactivation rate, %	EID_{50}
Wall	>4.00	>99.99	5.50
Top of cabinet	>4.00	>99.99	
Table top 1	>4.00	>99.99	
Table top 1	>4.00	>99.99	
Chair armrest 1	>4.00	>99.99	
Chair armrest 2	>4.00	>99.99	
On the floor	4.00	99.99	

Table 4
Results of the third inactivation test IAVs.

Sample location	Deactivation logarithm, log R	Inactivation rate, %	EID_{50}
Wall	>4.00	>99.99	5.67
Top of cabinet	>4.00	>99.99	
Table top 1	>4.00	>99.99	
Table top 1	>4.00	>99.99	
Chair armrest 1	>4.00	>99.99	
Chair armrest 2	>4.00	>99.99	
On the floor	4.00	99.99	

to the six sample points directly exposed to the deep ultraviolet robot, the overall inactivation rate of IAVs was 99.99 %.

The objective of this study was to assess the suitability of the deep ultraviolet robot for use in classroom environments. To replicate a classroom setting, the experiment incorporated items commonly found in classrooms, such as blackboards and cabinets. Two control groups were established, namely the desktop control group and the chair arm control group. Following irradiation by the deep ultraviolet robot, both desktop 1 and desktop 2 exhibited an inactivation rate of ≥99.99 % for IAVs. The same results were observed for chair armrest 1 and chair armrest 2, consistent with the findings of the desktop control group. The movement of the deep ultraviolet robot for 10 min resulted in an inactivation logarithm of ≥4log for IAVs. Similarly, the tests conducted on the blackboard and the top of the cabinet yielded comparable outcomes. Furthermore, analysis of the UVC lamp's optical power density curve indicated that when the density reached 1.6 mW/cm^2, the robot effectively and rapidly inactivated the IAVs, Fig. 2(a). Therefore, the experimental results show that the GXU robot can inactivate the H1N1 virus in a simulated classroom environment. This provides further evidence that the robot can inactivate influenza A viruses in a classroom environment.

5. Limitations and perspectives

Since the emergence of the COVID-19 pandemic, deep-ultraviolet robots have emerged as a solution to address the challenges associated with manual disinfection procedures [22,23]. Extensive research has highlighted the limitations of manual disinfection, including a surface virus clearance rate of less than 50 % [24–26], the potential risk of virus transmission to cleaning personnel [27], and environmental pollution caused by disinfectants [28,29]. In contrast, deep ultraviolet robots offer a non-contact disinfection approach that automates the germicidal process, eliminating the need for direct contact between cleaning personnel and the virus [30]. Furthermore, in real-world settings, deep ultraviolet robots demonstrate superior and faster virus inactivation capabilities on object surfaces [24].

Nevertheless, the practical application of deep ultraviolet robots in settings, such as hospitals, classrooms and bus stations, remains limited. This is primarily due to the potential harm posed by both mercury lamps and the UVC lamps used in this study to human health. Prolonged exposure to UVC radiation can lead to various adverse effects on the human body, including the development of conditions like cataracts [31]. Consequently, it is essential to ensure that the surrounding environment is free of individuals when the deep ultraviolet robot is in operation. This significant limitation significantly restricts the usage time and range of the deep ultraviolet robot.

The introduction of far UVC technology offers a potential solution to this predicament. Extensive research indicates that far UVC radiation poses minimal harm to the human body [32–34]. Both human skin and eyes can be directly exposed to far UVC without experiencing any damage [16,34]. Furthermore, numerous studies have demonstrated the efficacy of far UVC in virus inactivation. For instance, David Welch et al. [16] found that far UVC (222 nm) can deactivate over 95 % of atomized H1N1 influenza virus at a remarkably low dose of 2 mJ/cm^2. K. Narita et al. [17] reported the absence of detectable IAVs when exposed to a radiation dose of 6 mJ/cm^2 of far-ultraviolet light (222 nm). Lv. M et al. [35] achieved a 99.9 % inactivation rate of *E. coli* on object surfaces at an irradiation dose of 12.8 mJ/cm^2 using a far ultraviolet excimer lamp. Additionally, Jung, WK et al. [36] demonstrated that far UVC can deactivate over 99.99 % of coronaviruses at a dose of less than 8 mJ/cm^2. Consequently, future research may focus on combining far UVC technology with robots to effectively inactivate bacteria in various environments.

6. Conclusion

Although restrictions on COVID-19 have been eased globally and societies are gradually returning to normal, the virus has not completely disappeared. After the relaxation of regulations, COVID-19 is still spreading rapidly, especially in crowded places such as schools, hospitals and stations. Governments continue to face challenges in managing COVID-19.

The IAVs has been a problem for environmental disinfection. In order to verify whether a robot can inactivate IAVs in complex environments, such as classrooms, this study conducted two experiments using a robot (GXU Robot) with a 273 nm UVC lamp and successfully demonstrated the feasibility of the robot to inactivate IAVs in a classroom environment. In the classroom experiment, it was demonstrated that the UV dose of GXU Robot was able to reach the standard for inactivating IAVs (3 mJ/cm^2) within 80 min, except for shaded areas such as the bottom of desks. Then, further simulated classroom experiments were conducted. The test results showed that GXU Robot was able to inactivate 99.99 % of IAVs in a short period of time (10 min) In addition, by analyzing the optical power density curve of the UV lamp, it was demonstrated that GXU Robot could inactivate IAVs at an optical power density of 1.6 mW/cm^2. The results of this research are applicable not only to classrooms, but also to hospitals and other environments. In addition, these findings provide insights for preventing the spread of novel tubule viruses and other viruses, as well as valuable information for future UV research efforts.

Ethics statement

This study used chicken embryos aged 9–11 days. After inoculation of Influenza A virus, the chicken embryos were cultured for 3 days, and did not exceed 2/3 of the embryo hatching.

Funding statement

This study was supported in part by National Key Research and Development Program (Nos. 2022YFB3605100 and 2022YFB3605101), Disinfection Robot Based on High Power AlGaN-based UVLEDs (No. BB31200014), Guangxi Science and Technology Program (No. AD19245132), Guangxi University Foundation (No. A3120051010), High luminous efficiency and long life DUV LED technology (No. AC22080003), the Natural Science Foundation of Guangxi Province (No. 2021JJA170187), Guangxi Science and Technology Base and Talent Special Project (No. 2021AC20026), the Natural Science Foundation of Guangxi (No. 2021GXNSFAA075005), Production Development of Epitaxial Wafers Grown by MOCVD (No. KY03000031224002).

Data availability statement

The data that support the findings of this study are available from the corresponding author upon reasonable request, including the Android mobile control app developed in this study. In addition, the data associated with this study was not stored in publicly available repositories.

CRediT authorship contribution statement

Yizhen Wu: Writing – review & editing, Writing – original draft, Project administration, Methodology, Investigation, Data curation. **Peiyao Guo:** Software. **Dekun Luo:** Software. **Jianyu Deng:** Writing – review & editing. **Huilu Yao:** Supervision, Funding acquisition. **Wenhong Sun:** Writing – review & editing, Supervision, Funding acquisition.

Declaration of competing interest

The authors declare that they have no known competing financial interests or personal relationships that could have appeared to influence the work reported in this paper.

Appendix ASupplementary data

See the supplementary materials on real-life classroom testing and simulated classroom in the office. Fig. S1 in the supplementary explanation for classroom testing. The numbers on Fig. S1(a) are the 10 position points (1, 2, 3, 4, 5, 6, 7, 8, 9, 10) and the GXU Robot path is determined by these numbers. When the robot moves, the motion task, i.e., the path, is set using the GXU Robot app, and the motion task is 1 → 2 → 3 → 4 → 5 → 6 → 7 → 8 → 9 → 10 → 1. Figs. S2–S4 in the supplementary explanation for Fig. 4 in the study Fig. S2(a)–(c) corresponding to the numbers 2, 3 and 6 in Fig. 3(b) in the study. Fig. S3(a)–(d) corresponding to the numbers 4, 5, 1 and 7 in Fig. 3(b) in the study. Fig. S4 corresponding to Fig. 3(b) in the study. Supplementary data to this article can be found online at https://doi.org/10.1016/j.heliyon.2024.e29540.

References

[1] China Bureau for Disease Control and Prevention. The National Bureau of Disease Control and Prevention Released an Overview of the National Epidemic Situation of Notifiable Infectious Diseases in August 2022. National Health Commission of the People's Republic of China(nhc.gov.cn)..

[2] Centers for Disease Control and Prevention. The United States of America. Disease 7 Bureau of Flu, Disease Burden of Flu, CDC, 2022.

[3] P. Vasickova, I. Pavlik, M. Verani, A. Carducci, Issues concerning survival of viruses on surfaces, Food Environ. Virol. 2 (2010) 24–34, https://doi.org/10.1007/s12560-010-9025-6.

[4] C. Lorca-Oro, J. Vila, P. Pleguezuelos, J. Vergara-Alert, J. Rodon, N. Majo, S. Lopez, J. Segales, F. Saldana-Buesa, M. Visa-Boladeras, A. Vea-Baro, J. M. Campistol, X. Abad, Rapid SARS-CoV-2 inactivation in a simulated hospital room using a mobile and autonomous robot emitting ultraviolet-C light, J. Infect. Dis. 225 (2022) 587–592, https://doi.org/10.1093/infdis/jiab551.

[5] L. Bennett, G. Waterer, Control measures for human respiratory viral infection, Semin. Respir. Crit. Care Med. 37 (2016) 631–639, https://doi.org/10.1055/s-0036-1584792.

[6] M. Khanna, N. Gupta, A. Gupta, V. Vijayan, Influenza A (H1N1) 2009: a pandemic alarm, J. Biosci. 34 (2009) 481–489, https://doi.org/10.1007/s12038-009-0053-z.

[7] S.J. Sullivan, R.M. Jacobson, W.R. Dowdle, G.A. Poland, 2009 H1N1 Influenza, in: Mayo Clinic Proceedings, Elsevier, 2010, pp. 64–76, https://doi.org/10.4065/mcp.2009.0588.

[8] J. Barker, D. Stevens, S. Bloomfield, Spread and prevention of some common viral infections in community facilities and domestic homes, J. Appl. Microbiol. 91 (2001) 7–21, https://doi.org/10.1046/j.1365-2672.2001.01364.x.

[9] J. Hofemeister, H. Boehme, M. Fleischhacker, B. Adler, G. Eitner, G. Steinborn, DNA repair in proteus mirabilis. 5, Biol. Zentralblatt 98 (1979) 315–332, https://doi.org/10.1007/BF00273221.

[10] A. Vink, P. Van den Berg, L. Roza, DNA damaoe, repair, and tannino acceleration, J. Cosmet. Sci. 50 (1999) 341–349.

[11] T. Lindahl, R.D. Wood, Quality control by DNA repair, Science 286 (1999) 1897–1905, https://doi.org/10.1126/science.286.5446.1897.

[12] S. Cooper, G. Bowden, Ultraviolet B regulation of transcription factor families: roles of nuclear factor-kappa B (NF-κB) and activator protein-1 (AP-1) in UVB-induced skin carcinogenesis, Curr. Cancer Drug Targets 7 (2007) 325–334, https://doi.org/10.2174/156800907780809714.

[13] W. Kong, F. Wang, B. Dong, C. Ou, D. Meng, J. Liu, Z.C. Fan, Novel reassortant influenza viruses between pandemic (H1N1) 2009 and other influenza viruses pose a risk to public health, Microb. Pathog. 89 (2015) 62–72, https://doi.org/10.1016/j.micpath.2015.09.002.

[14] D. Mills, D.A. Harnish, C. Lawrence, M. Sandoval-Powers, B.K. Heimbuch, Ultraviolet germicidal irradiation of influenza-contaminated N95 filtering facepiece respirators, Am. J. Infect. Control 46 (2018) e49–e55, https://doi.org/10.1016/j.ajic.2018.02.018.

[15] M. Kojima, K. Mawatari, T. Emoto, R. Nishisaka-Nonaka, T.K.N. Bui, T. Shimohata, T. Uebanso, M. Akutagawa, Y. Kinouchi, T. Wada, M. Okamoto, H. Ito, K. Tojo, T. Daidoji, T. Nakaya, A. Takahashi, Irradiation by a combination of different peak-wavelength ultraviolet-light emitting diodes enhances the inactivation of influenza A viruses, Microorganisms 8 (2020), https://doi.org/10.3390/microorganisms8071014.

[16] D. Welch, M. Buonanno, V. Grilj, I. Shuryak, C. Crickmore, A.W. Bigelow, G. Randers-Pehrson, G.W. Johnson, D.J. Brenner, Far-UVC light: a new tool to control the spread of airborne-mediated microbial diseases, Sci. Rep. 8 (2018) 2752, https://doi.org/10.1038/s41598-018-21058-w.

[17] K. Narita, K. Asano, K. Naito, H. Ohashi, M. Sasaki, Y. Morimoto, T. Igarashi, A. Nakane, 222-nm UVC inactivates a wide spectrum of microbial pathogens, J. Hosp. Infect. (2020), https://doi.org/10.1016/j.jhin.2020.03.030.

[18] C. McGinn, R. Scott, N. Donnelly, K.L. Roberts, M. Bogue, C. Kiernan, M. Beckett, Exploring the applicability of robot-assisted UV disinfection in radiology, Front. Robot AI 7 (2020) 590306, https://doi.org/10.3389/frobt.2020.590306.

[19] A.E. Martinez de Alba, M.B. Rubio, M.E. Moran-Diez, C. Bernabeu, R. Hermosa, E. Monte, Microbiological evaluation of the disinfecting potential of UV-C and UV-C plus ozone generating robots, Microorganisms 9 (2021), https://doi.org/10.3390/microorganisms9010172.

[20] F. Astrid, Z. Beata, M. Van den Nest, E. Julia, P. Elisabeth, D.E. Magda, The use of a UV-C disinfection robot in the routine cleaning process: a field study in an Academic hospital, Antimicrob. Resist. Infect. Control 10 (2021) 84, https://doi.org/10.1186/s13756-021-00945-4.

[21] L. Tiseni, D. Chiaradia, M. Gabardi, M. Solazzi, D. Leonardis, A. Frisoli, UV-C mobile robots with optimized path planning: algorithm design and on-field measurements to improve surface disinfection against SARS-CoV-2, IEEE Robot. Autom. Mag. 28 (2021) 59–70, https://doi.org/10.1109/mra.2020.3045069.

[22] M. Diab-El Schahawi, W. Zingg, M. Vos, H. Humphreys, L. Lopez-Cerero, A. Fueszl, J.R. Zahar, E. Presterl, E.S.G.o.N.I.T.d.r.w. group, Ultraviolet disinfection robots to improve hospital cleaning: real promise or just a gimmick? Antimicrob. Resist. Infect. Control 10 (2021) 33 https://doi.org/10.1186/s13756-020-00878-4.

[23] S.D. Sierra Marin, D. Gomez-Vargas, N. Cespedes, M. Munera, F. Roberti, P. Barria, S. Ramamoorthy, M. Becker, R. Carelli, C.A. Cifuentes, Expectations and perceptions of healthcare professionals for robot deployment in hospital environments during the COVID-19 pandemic, Front. Robot AI 8 (2021) 612746, https://doi.org/10.3389/frobt.2021.612746.

[24] P.C. Carling, Evaluating the thoroughness of environmental cleaning in hospitals, J. Hosp. Infect. 68 (2008) 273–274, https://doi.org/10.1016/j.jhin.2007.10.023.

[25] S.J. Dancer, Importance of the environment in meticillin-resistant Staphylococcus aureus acquisition: the case for hospital cleaning, Lancet Infect. Dis. 8 (2008) 101–113, https://doi.org/10.1016/S1473-3099(07)70241-4.

[26] P.C. Carling, M.M. Parry, M.E. Rupp, J.L. Po, B. Dick, S. Von Beheren, G. Healthcare Environmental Hygiene Study, Improving cleaning of the environment surrounding patients in 36 acute care hospitals, Infect. Control Hosp. Epidemiol. 29 (2008) 1035–1041, https://doi.org/10.1086/591940.

[27] G.-Z. Yang, B.J. Nelson, R.R. Murphy, H. Choset, H. Christensen, S.H. Collins, P. Dario, K. Goldberg, K. Ikuta, N. Jacobstein, Combating COVID-19—the role of robotics in managing public health and infectious diseases, in: American Association for the Advancement of Science, 2020 eabb5589, https://doi.org/10.1126/scirobotics.abb5589.

[28] W. de Bruin, M.C. van Zijl, N.H. Aneck-Hahn, L. Korsten, Quality and safety of South African hand sanitisers during the COVID-19 pandemic, Int. J. Environ. Health Res. (2023) 1–13, https://doi.org/10.1080/09603123.2023.2166020.

[29] R.S. Hussein, Hand sanitizers containing alcohol and their effects on the skin during the COVID-19 pandemic, Int. J. Biomed. 12 (2022) 204–208, https://doi.org/10.21103/Article12(2)_RA6.

[30] J.A. Otter, S. Yezli, T.M. Perl, F. Barbut, G.L. French, The role of 'no-touch' automated room disinfection systems in infection prevention and control, J. Hosp. Infect. 83 (2013) 1–13, https://doi.org/10.1016/j.jhin.2012.10.002.

[31] D. Balasubramanian, Ultraviolet radiation and cataract, J. Ocul. Pharmacol. Therapeut. 16 (2000) 285–297, https://doi.org/10.1089/jop.2000.16.285.

[32] M. Buonanno, G. Randers-Pehrson, A.W. Bigelow, S. Trivedi, F.D. Lowy, H.M. Spotnitz, S.M. Hammer, D.J. Brenner, 207-nm UV light - a promising tool for safe low-cost reduction of surgical site infections. I: in vitro studies, PLoS One 8 (2013) e76968, https://doi.org/10.1371/journal.pone.0076968.

[33] M. Buonanno, M. Stanislauskas, B. Ponnaiya, A.W. Bigelow, G. Randers-Pehrson, Y. Xu, I. Shuryak, L. Smilenov, D.M. Owens, D.J. Brenner, 207-nm UV light-A promising tool for safe low-cost reduction of surgical site infections. II: in-vivo safety studies, PLoS One 11 (2016) e0138418, https://doi.org/10.1371/journal.pone.0138418.

[34] M. Buonanno, B. Ponnaiya, D. Welch, M. Stanislauskas, G. Randers-Pehrson, L. Smilenov, F.D. Lowy, D.M. Owens, D.J. Brenner, Germicidal efficacy and mammalian skin safety of 222-nm UV light, Radiat. Res. 187 (2017) 483–491, https://doi.org/10.1667/RR0010CC.1.

[35] M. Lv, J. Huang, H. Chen, T.T. Zhang, An excimer lamp to provide far-ultraviolet C irradiation for dining-table disinfection, Sci. Rep. 13 (2023) 381, https://doi.org/10.1038/s41598-023-27380-2.

[36] W.K. Jung, K.T. Park, K.S. Lyoo, S.J. Park, Y.H. Park, Demonstration of antiviral activity of far-UVC microplasma lamp irradiation against SARS-CoV-2, Clin. Lab. 67 (2021), https://doi.org/10.7754/Clin.Lab.2020.201140.